Arteriosclerosis, Thrombosis, and Vascular Biology

BASIC SCIENCES

Macrophage ALDH2 (Aldehyde Dehydrogenase 2) Stabilizing Rac2 Is Required for Efferocytosis Internalization and Reduction of Atherosclerosis Development

Jian Zhang,* Xiangkai Zhao,* Yunyun Guo, Zhiping Liu, Shujian Wei, Qiuhuan Yuan, Haixia Shang, Wentao Sang, Sumei Cui, Tonghui Xu, Kehui Yang, Jialin Guo, Chang Pan, Jiali Wang, Jiaojiao Pang, Tianrui Han, Yuguo Chen, Feng Xu

BACKGROUND: Clinical studies show that the most common single-point mutation in humans, ALDH2 (aldehyde dehydrogenase 2) rs671 mutation, is a risk factor for the development and poor prognosis of atherosclerotic cardiovascular diseases, but the underlying mechanism remains unclear. Apoptotic cells are phagocytosed and eliminated by macrophage efferocytosis during atherosclerosis, and enhancement of arterial macrophage efferocytosis reduces atherosclerosis development.

METHODS: Plaque areas, necrotic core size, apoptosis, and efferocytosis in aortic lesions were investigated in APOE$^{-/-}$ mice with bone marrow transplanted from APOE$^{-/-}$ALDH2$^{-/-}$ and APOE$^{-/-}$ mice. RNA-seq, proteomics, and immunoprecipitation experiments were used to screen and validate signaling pathways affected by ALDH2. Efferocytosis and protein levels were verified in human macrophages from wild-type and rs671 mutation populations.

RESULTS: We found that transplanting bone marrow from APOE$^{-/-}$ALDH2$^{-/-}$ to APOE$^{-/-}$ mice significantly increased atherosclerosis plaques compared with transplanting bone marrow from APOE$^{-/-}$ to APOE$^{-/-}$ mice. In addition to defective efferocytosis in plaques of APOE$^{-/-}$ mice bone marrow transplanted from APOE$^{-/-}$ALDH2$^{-/-}$ mice in vivo, macrophages from ALDH2$^{-/-}$ mice also showed significantly impaired efferocytotic activity in vitro. Subsequent RNA-seq, proteomics, and immunoprecipitation experiments showed that wild-type ALDH2 directly interacted with Rac2 and attenuated its degradation due to decreasing the K48-linked polyubiquitination of lysine 123 in Rac2, whereas the rs671 mutant markedly destabilized Rac2. Furthermore, Rac2 played a more crucial role than other Rho GTPases in the internalization process in which Rac2 was up-regulated, activated, and clustered into dots. Overexpression of wild-type ALDH2 in ALDH2$^{-/-}$ macrophages, rather than the rs671 mutant, rescued Rac2 degradation and defective efferocytosis. More importantly, ALDH2 rs671 in human macrophages dampened the apoptotic cells induced upregulation of Rac2 and subsequent efferocytosis.

CONCLUSIONS: Our study has uncovered a pivotal role of the ALDH2-Rac2 axis in mediating efferocytosis during atherosclerosis, highlighting a potential therapeutic strategy in cardiovascular diseases, especially for ALDH2 rs671 mutation carriers.

GRAPHIC ABSTRACT: A graphic abstract is available for this article.

Key Words: apoptosis ■ atherosclerosis ■ macrophage ■ proteomics

The advanced atherosclerotic plaques lead to acute coronary syndromes (ACS), which are the leading cause of morbidity and mortality worldwide.[1] Macrophages play a central role in advanced plaque formation. Increasing evidence shows that arterial macrophage efferocytosis (ability to uptake apoptotic cells) plays a pivotal role in

Correspondence to: Feng Xu, MD, PhD, Department of Emergency Medicine, Qilu Hospital, Shandong University, 107 Wenhuaxi Rd, Jinan 250012, China. Email xufengsdu@126.com
*J. Zhang and X. Zhao contributed equally.
Supplemental Material is available at https://www.ahajournals.org/doi/suppl/10.1161/ATVBAHA.121.317204.
For Sources of Funding and Disclosures, see page 715.

Arterioscler Thromb Vasc Biol is available at www.ahajournals.org/journal/atvb

Nonstandard Abbreviations and Acronyms

ACS	acute coronary syndrome
ALDH2	aldehyde dehydrogenase 2
BMDMs	bone-marrow derived macrophages
HDL	high-density lipoprotein
LDL	low-density lipoprotein
PBMCs	peripheral blood mononuclear cells
VSMCs	vascular smooth muscle cells
α-SMA	α-smooth muscle actin

atherosclerotic lesion development and establishment of the necrotic core.[2] Defective efferocytosis leads to secondary necrosis of apoptotic cells and enlargement of the necrosis core, which promotes atherosclerosis and increases the risk of ACS occurrence. Therefore, enhancement of macrophage efferocytotic ability represents a feasible strategy to regress atherosclerosis and stabilize plaques.[3–6] The process of efferocytosis consists of 3 stages, apoptotic cell finding, binding, and internalization and degradation.[4] Translational therapeutic strategies based on the finding and binding stages, such as increasing MERTK (MER receptor tyrosine kinase) levels or using anti-CD47 antibodies, have been associated with side effects including inflammation suppression and erythrophagocytosis.[4,6] The search for therapeutic approaches has therefore shifted to targeting the internalization and degradation stage of efferocytosis.[4]

See accompanying editorial on page 717
See cover image

ALDH2 (aldehyde dehydrogenase 2) gene mutation is a concerning latent risk factor for cardiovascular diseases.[7–9] The inactivating mutation of ALDH2 (termed ALDH2*2 or rs671 mutant) generally only influences East Asian populations,[10] and it may be the most common human enzyme deficiency and affecting ≈560 million people worldwide in contrast to the ≈400 million people with the well-known mutation of glucose-6-phosphate dehydrogenase.[11] Our clinical studies had demonstrated the relationships between rs671 mutation and increased ACS incidence and worse prognosis,[12,13] however, the underlying molecular mechanism remained unclear. We posited that ALDH2 in macrophages plays an unrecognized key role in the internalization process of efferocytosis and stability of advanced plaques.

In the present study, we revealed that bone marrow transplantation from APOE$^{-/-}$ALDH2$^{-/-}$ to APOE$^{-/-}$ mice markedly aggravated atherosclerosis compared with bone marrow transplantation from APOE$^{-/-}$ to APOE$^{-/-}$ mice. By means of RNA-seq and proteomics, we innovatively discovered that ALDH2 directly interacted with Rac2 and regulated ubiquitination of the latter, subsequently availing macrophage efferocytosis. Our study demonstrated a novel mechanism for atherosclerosis management based on the ALDH2-Rac2-efferocytosis axis which constitutes a potential new therapeutic target.

Highlights

- Transplanting bone marrow of APOE$^{-/-}$ALDH2$^{-/-}$ mice to APOE$^{-/-}$ mice accelerates atherosclerosis development.
- ALDH2 (aldehyde dehydrogenase 2) stabilizes Rac2, subsequently facilitating macrophage efferocytosis and preventing atherosclerosis.
- ALDH2 interacts with Rac2 and regulates K48-linked polyubiquitination of the latter at K123.
- Enhancement of Rac2 expression may be beneficial for atherosclerosis prevention, especially for ALDH2 rs671 mutation populations.

MATERIALS AND METHODS

Availability of Data and Material

The data that support the findings of this study are available from the corresponding author upon reasonable request.

Mice

Male 6 to 8-week-old ALDH2$^{-/-}$APOE$^{-/-}$, APOE$^{-/-}$, ALDH2$^{-/-}$, and C57BL/6J (wild-type) mice, and their littermates were used in our study. ALDH2$^{-/-}$APOE$^{-/-}$ mice were generated in our laboratory. ALDH2$^{-/-}$ mice were provided by University of Occupational and Environmental Health (Fukuoka, Japan). ALDH2$^{-/-}$ mice were constructed on a C57BL/6J background of the same strain and backcrossed for at least 10 generations with in-house C57BL/6J mice to create a congenic strain. After backcross, ALDH2$^{+/-}$APOE$^{+/-}$ were mated separately to generate control and experimental groups of mice. The study was performed only with male mice, as there is study reporting that atherosclerotic plaques develop more reproducibly and with less biological variability.[14] And we intended to avoid the influence of estrogen in female mice. Sample size for each experiment is described in the figure legends section. No randomization or blinding methods were used for animal studies. The study was adhered to the guideline for experimental atherosclerosis studies described in the Scientific Statement from the American Heart Association[15] and the guidelines as described in the ATVB Council Statement.[16] All animal procedures were in accordance with the National Institutes of Health Guidelines for the care and use of laboratory animals and were approved by the Animal Use and Care Committee of Shandong University.

Human Subjects

We used the Ficoll density gradient (catalog 17-1440-02, BD Biosciences) to isolate human peripheral blood mononuclear cells (PBMCs) according to the protocols. Then, PBMCs were treated with differentiated medium (RPMI-1640, 10% FBS, 25

ng/mL hM-CSF (human macrophage colony-stimulating factor 1)) for 10 days to differentiate macrophages. This study was approved by the Ethics Committee of Shangdong University, Shangdong, China.

Bone Marrow Transplantation

The mice were lethally irradiated (8.5Gy with X-ray), then injected IV (tail vein) with 1×10^7 bone marrow cells from donor mice for bone marrow transplantation as previously described.[17] Briefly, one day before and 2 days after the transplantation, mice were fasted and fed with DMEM culture medium intragastrically. During the recovery phase of 4 weeks, mice were fed with water containing sulfamethoxazole (200 mg/mL) and trimethoprim (40 mg/mL). After recovery, mice were fed a high-fat diet for 8 weeks. APOE$^{-/-}$ mice and ALDH2$^{-/-}$APOE$^{-/-}$ mice were used as bone marrow donors to reconstitute lethally irradiated APOE$^{-/-}$ mice.

Animal Anesthesia, Euthanasia, and Tissue Collection

At the end of animal experiment, anesthesia was induced and maintained throughout the whole procedure with isoflurane (4% isoflurane/0.2 L O_2/min for induction, and 2% isoflurane/0.2 L O_2/min for maintenance). In the end, all mice were euthanized by cervical dislocation. After collecting blood by cardiac puncture, the vascular perfusion was performed with PBS solution. After perfusion, the heart and aorta were dissected and preserved for further analysis.

Atherosclerotic Lesion Characterization, Histological, and Immunofluorescence Analysis

Aortic roots were embedded in optimum cutting temperature reagents and aortic root serial sections were prepared to analyze atherosclerotic lesions. Lesion areas in aortic roots were shown as the ratio of plaque area/total lumen area. To determine atherosclerotic lesion sizes, we stained the aortic root sections with hematoxylin-eosin staining. To determine the components of the plaque, we used oil red O, α-SMA (α-smooth muscle actin), anti-monocyte+macrophage antibody, and Sirius red staining, and data are shown as the value of positive area of staining/plaque area.

Reagents

Adenovirus, lentivirus, and siRNA used in this study were constructed and sequenced to confirm their identity. ALDH2, rs671 and Rac2 plasmid, LV-ALDH2, and LV-rs671 were purchased from Genechem (Shanghai, China). HA-tagged ubiquitin and other plasmids were kept in our laboratory. The siRNA-Rac2 was obtained from GenePharma (Shanghai, China) and the sequence was as follows: 5'-CCACUGUAUUUGACAACUATT-3'. The scrambled siRNA together with transfection reagents was used as the negative control. Fluorescein amidite-labeled scrambled siRNA was used as fluorescence control. The antibodies used in the study were shown in the Major Resources Table.

Efferocytosis Assay

For efferocytosis assay in vitro, primary mouse vascular smooth muscle cells (VSMCs), primary peritoneal macrophages, and bone-marrow derived macrophages (BMDMs) were extracted and cultured. Mice were anesthetized with isoflurane (4% isoflurane/0.2 L O_2/min) and then euthanized by cervical dislocation. BMDMs were generated as previously described.[17] Briefly, bone marrow cells were flushed from the tibia and femurs of 6- to 8-week-old ALDH2$^{-/-}$ or C57BL/6J mice. Cells were cultured in DMEM supplemented with 10% FBS (Gibco), and 1% penicillin-streptomycin (Gibco) and stimulated with 25 ng/mL mouse M-CSF (macrophage colony-stimulating factor 1; Biolegend) for 6 days. Mouse peritoneal macrophages from ALDH2$^{-/-}$ and C57BL/6J mice were isolated 3 days after intraperitoneal injection with a 4% thioglycolate solution (Sigma Aldrich), as previously described.[18] VSMCs from mouse aortas (stripped of adventitia) were isolated by enzymatic digestion and grown in DMEM with 10% FBS as described previously.[8] Cells from passages 4 to 8 were grown to around 80% confluence for experiments. Primary VSMCs were stained with CellTracker Deep Red dye (Invitrogen, C34565) in a 1:1000 dilution and then incubated with 1 μmol/L staurosporine for 6 hours to induce apoptosis. The apoptosis rate of induced VSMCs was >80% assessed by flow cytometry using FITC Annexin V Apoptosis Detection Kit I (BD biosciences, 556547). The apoptotic VSMCs were scraped off and underwent cell counting. After cell counting, the apoptotic cells were added into peritoneal macrophages or BMDMs in a 1:1 ratio for 90 minutes.[19,20] The free apoptotic cells were washed off, and the macrophages were collected to undergo flow cytometry after being stained with anti-F4/80 antibody. Double-positive cells for Deep Red and F4/80 were considered as efferocytotic macrophages. And the efferocytotic rate was calculated as (Double-positive cells)/(All F4/80 positive cells). Jurkat cells were stained with CellTracker Deep Red dye (Invitrogen, C34565) in a 1:1000 dilution. After staining, Jurkat cells were irradiated under the UV lamp for 20 minutes and were cultured under the normal condition for 3 hours. After cell counting, the apoptotic Jurkat cells were added into human PBMCs in a 1:1 ratio for 90 minutes, and free apoptotic cells were washed out before collection for flow cytometry. Human PBMCs were labeled with anti-human CD68 phycoerythrin-conjugated antibody. The efferocytosis rate was shown as the value of (double-positive cells)/(all phycoerythrin positive cells).

Western Blotting and Immunofluorescence Staining

Primary peritoneal macrophages and BMDMs were stimulated with apoptotic cells for 90 minutes in a 1:5 ratio (macrophages: apoptotic cells=1:5), and the free apoptotic cells were washed out before collection. As for degradation analysis of Rac2 in Figure 6A and 6B, peritoneal macrophages were stimulated with apoptotic cells for 90

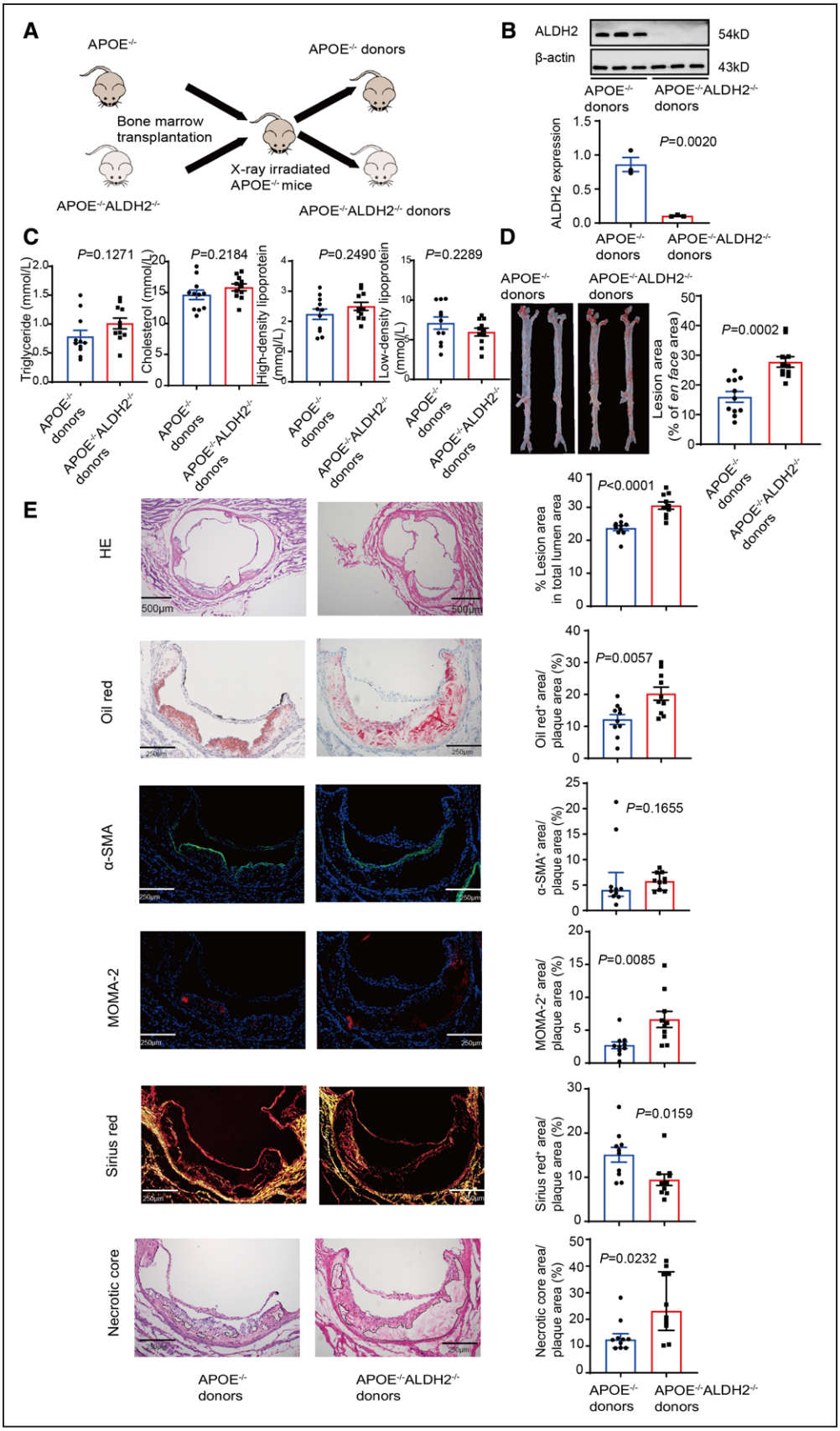

Figure 1. Bone marrow transplantation from APOE$^{-/-}$ALDH2$^{-/-}$ mice into APOE$^{-/-}$ mice accelerates atherosclerosis.
A, Procedure diagram of bone marrow transplantation. **B**, After the bone marrow transplantation experiment procedure, primary peritoneal macrophages were extracted from APOE$^{-/-}$ mice transplanted with APOE$^{-/-}$ bone marrow and APOE$^{-/-}$ mice transplanted (*Continued*)

minutes. Human PBMCs were stimulated with apoptotic Jurkat cells for 90 minutes (macrophages: apoptotic cells=1:5), and the free apoptotic cells were washed out before collection. To induce apoptosis, Jurkat cells were irradiated under the UV lamp for 20 minutes and cultured under normal conditions for 3 hours. The apoptosis rate of induced Jurkat cells was >80% as assessed by flow cytometry using FITC Annexin V Apoptosis Detection Kit I (BD biosciences, 556547). Colocalization of Rac2 and ALDH2 was analyzed with the plug in coloc2 for image J and Manders' Colocalization Coefficients were used to estimate colocalization as previously described.[21,22]

Live-Cell Imaging System

Primary peritoneal macrophages were placed onto a glass-bottom culture plate and stained with CellTracker Deep Red dye (Invitrogen, C34565). Primary VSMCs were stained with CellTracker Green CMFDA dye (Invitrogen, C2925) and incubated with 1 μmol/L staurosporine for 6 hours. After adding apoptotic VSMCs into macrophages, the plate was immediately placed into the confocal scanner box (PerkinElmer, Opera Phenix) featuring a culture system maintained at 37 °C and 5% CO_2. The fluorescence images were acquired using a 63×objective lens at a 2-minute interval, lasting for 120 minutes.

In Vitro Binding Assay

Flag-ALDH2, Flag-rs671, and Myc-Rac2 proteins were expressed with a TNT Quick Coupled Transcription/Translation System (Promega) according to the instructions of the manufacturer. Flag-ALDH2 or Flag-rs671 were mixed with Myc-Rac2 in the lysis buffer and then were immunoprecipitated before being subjected to immunoblots with the indicated antibodies.

Code Availability

Raw data (ID GSE156234) was downloaded from GEO data set[23]; Seurat package[24] was used to preprocess the single-cell data and further find the differential marker genes between the 2 different states.

Statistical Analysis

All data were analyzed for normality and equal variance. Data were shown as the mean±SE of mean when they passed normality test and analyzed by the 2-tailed Student *t* test or 1-way ANOVA followed by the Tukey post hoc test. When the data did not pass normality test, they were shown as the median (second quartile, third quartile) and analyzed by Mann-Whitney test or Kruskal-Wallis test followed by the Dunn post hoc test. All data were analyzed using the GraphPad Prism 8 software (GraphPad, La Jolla, CA). No statistic method was used to calculate sample size, and no sample values were excluded during analysis. Statistical significance was accepted when *P* value was <0.05.

RESULTS

Bone Marrow Transplantation From APOE$^{-/-}$ALDH2$^{-/-}$ Mice Into APOE$^{-/-}$ Mice Accelerates Atherosclerosis

To testify whether macrophage ALDH2 plays a key role in formation of advanced plaques, we used bone marrow transplantation to generate ALDH2 bone marrow chimeric mice (Figure 1A). Deletion of ALDH2 was validated in elicited peritoneal macrophages by Western blotting (Figure 1B). ALDH2 deletion in bone marrow cells did not alter the concentration of triglyceride, cholesterol, HDL (high-density lipoprotein), and LDL (low-density lipoprotein) in serum between the 2 groups (Figure 1C). To examine the effect of ALDH2 on atherosclerotic development, the total areas of aortas were measured using oil red O staining, and sections of aortic root using HE staining. Results showed that transplanting bone marrow from APOE$^{-/-}$ALDH2$^{-/-}$ to APOE$^{-/-}$ mice significantly enlarged atherosclerotic plaque areas compared with transplanting bone marrow from APOE$^{-/-}$ to APOE$^{-/-}$ mice, both in the aortas and aortic root (27.7±1.8% versus 15.9±1.8%, *P*=0.0002; 30.5±1.1% versus 23.7±0.8%, *P*<0.0001, respectively, Figure 1D and 1E). The lipid accumulation and macrophage infiltration were significantly increased in the APOE$^{-/-}$ mice transplanted with APOE$^{-/-}$ALDH2$^{-/-}$ bone marrow compared with the APOE$^{-/-}$ mice transplanted with APOE$^{-/-}$ bone marrow, while collagen contents were decreased. Oil red O staining showed that APOE$^{-/-}$ mice transplanted with APOE$^{-/-}$ALDH2$^{-/-}$ bone marrow accumulated more lipid than APOE$^{-/-}$ mice transplanted with APOE$^{-/-}$ bone marrow (20.2±2.1% versus 12.2±0.2%, *P*=0.0057, Figure 1E). A significant increase of infiltrated inflammatory macrophages was found in APOE$^{-/-}$ mice transplanted with APOE$^{-/-}$ALDH2$^{-/-}$ bone marrow compared with APOE$^{-/-}$ mice transplanted with APOE$^{-/-}$ bone marrow (6.6±1.2% versus 2.7±0.5%, *P*=0.0085, Figure 1E). In contrast, the collagen^{+} components in plaques were markedly decreased in APOE$^{-/-}$ mice transplanted with APOE$^{-/-}$ALDH2$^{-/-}$ bone marrow compared with APOE$^{-/-}$ mice transplanted with APOE$^{-/-}$ bone marrow

Figure 1 Continued. with APOE$^{-/-}$ALDH2$^{-/-}$ bone marrow to verify the bone marrow clearance efficiency (n=3). **C**, After 4-week recovery and 8-week high-fat diet, APOE$^{-/-}$ mice transplanted with APOE$^{-/-}$ALDH2$^{-/-}$ bone marrow and APOE$^{-/-}$ mice transplanted with APOE$^{-/-}$ bone marrow were euthanized and serum was used to detect triglyceride, cholesterol, HDL (high-density lipoprotein), and LDL (low-density lipoprotein; **C**, n=11). **D**, Representative en face photographs of aortas showing oil red O-stained atherosclerotic plaques (n=11). **E**, Representative photographs of HE staining, oil red O staining, α-SMA immunofluorescence staining, anti-monocyte+macrophage antibody (MOMA2) immunofluorescence staining, Sirius red staining and necrotic cores of frozen sections of the tricuspid valve and their statistic graphs (n=10). Data were shown as the mean±SE of mean and Student *t* test was used for statistical analysis, if not specifically indicated. As for α-SMA immunofluorescence staining and necrotic cores, data were analyzed by Mann-Whitney test.

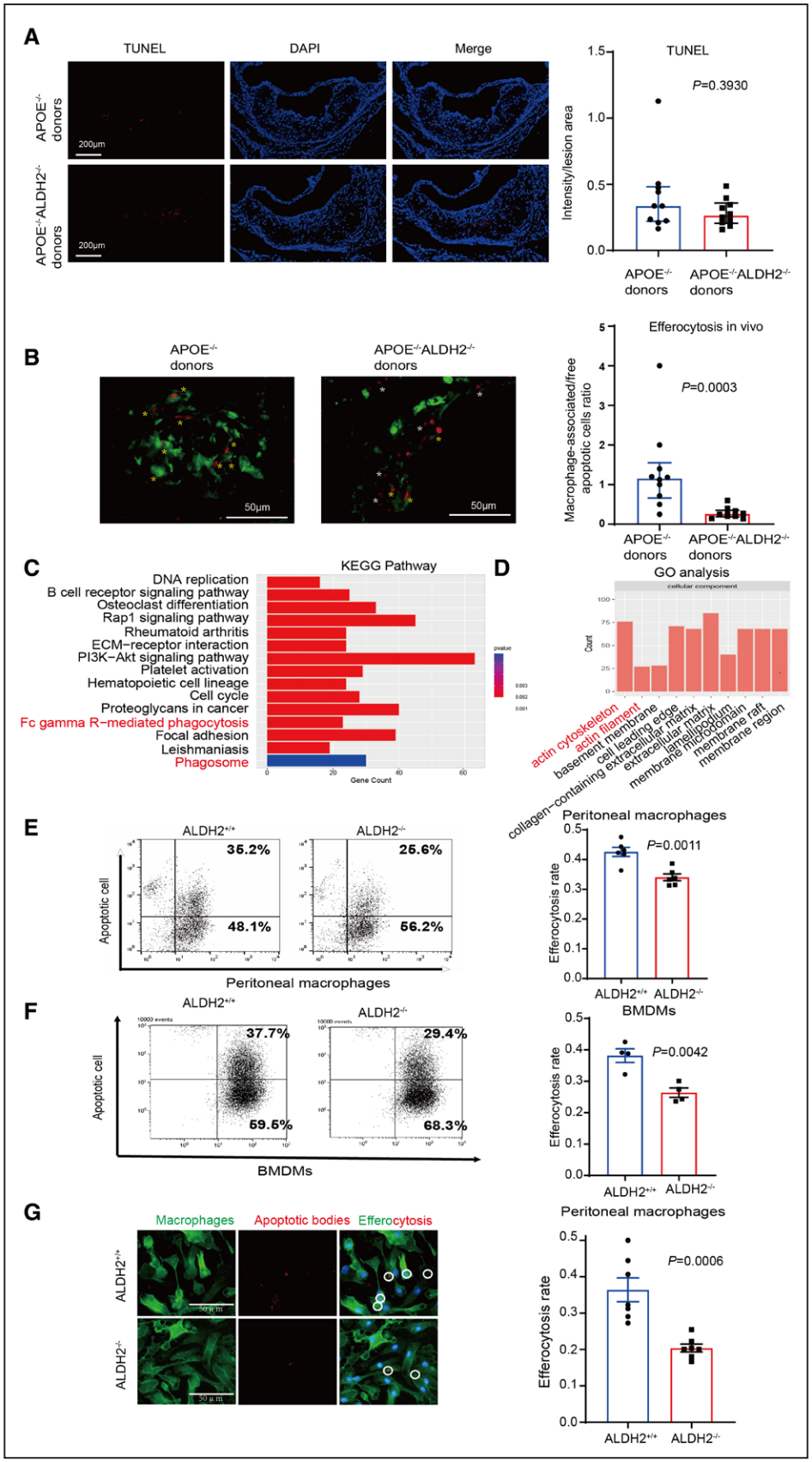

Figure 2. ALDH2 (aldehyde dehydrogenase 2) deletion dampens macrophage efferocytosis function in vivo and in vitro.
A, TdT-mediated dUTP Nick-End Labeling (TUNEL) staining of frozen sections of the tricuspid valve from APOE$^{-/-}$ mice transplanted with APOE$^{-/-}$ bone marrow and APOE$^{-/-}$ mice transplanted with APOE$^{-/-}$ALDH2$^{-/-}$ bone marrow which were fed with high-fat diet for 8 wk. (*Continued*)

(9.4±1.3% versus 15.1±1.7%, *P*=0.0159; Figure 1E). The α-SMA$^+$ components in plaques showed no statistic difference between APOE$^{-/-}$ mice transplanted with APOE$^{-/-}$ALDH2$^{-/-}$ bone marrow and APOE$^{-/-}$ mice transplanted with APOE$^{-/-}$ bone marrow (5.7% [4.0%–7.5%] versus 4.0% [2.8%–7.5%], *P*=0.1655; Figure 1E). Importantly, significantly enlarged necrotic cores were shown in APOE$^{-/-}$ mice transplanted with APOE$^{-/-}$ALDH2$^{-/-}$ bone marrow compared with APOE$^{-/-}$ mice transplanted with APOE$^{-/-}$ bone marrow (23.1% [15.9%–37.8%] versus 12.4 [9.3%–14.6%], *P*=0.0232; Figure 1E). Collectively, these data demonstrated that bone marrow transplantation from APOE$^{-/-}$ALDH2$^{-/-}$ mice into APOE$^{-/-}$ mice contributed to advanced plaques, which may be related to macrophage efferocytosis.

ALDH2 Deletion Dampens Macrophage Efferocytosis Function In Vivo and In Vitro

To investigate the underlying mechanism by which ALDH2 deficiency in bone marrow cells resulted in larger necrotic cores, we focus on cell apoptosis and efferocytosis, which mainly contributes to the necrotic cores. Interestingly, the total apoptotic cells between the 2 groups were comparable (26.3% [20.5%–35.8%] versus 33.6% [22.0%–48.1%], *P*=0.3930; Figure 2A), when detected with TdT-mediated dUTP Nick-End Labeling. Furthermore, in advanced plaque regions of aortic root sections from mice fed with high-fat diet, we used immunofluorescence and TdT-mediated dUTP Nick-End Labeling staining to detect efferocytosis. The ratio of macrophage-associated apoptotic cells to free apoptotic cells of APOE$^{-/-}$ mice transplanted with APOE$^{-/-}$ bone marrow was significantly higher than that of APOE$^{-/-}$ mice transplanted with APOE$^{-/-}$ALDH2$^{-/-}$ bone marrow (1.15 [0.66–1.55] versus 0.26 [0.19–0.35], *P*=0.0003; Figure 2B), suggesting that ALDH2 influenced macrophage efferocytosis and led to enlarged necrotic cores. To further verify the effect of ALDH2 on macrophage efferocytosis in vitro, we stimulated primary peritoneal macrophages from ALDH2$^{-/-}$ mice or wild-type mice with induced apoptotic VSMCs and analyzed mRNA expression patterns. The mixture of RNA-seq samples contained few apoptotic VSMCs because of the greatly lower expression of Myosin compared with CD14 and CD68 (Figure S1A). Kyoto Encyclopedia of Genes and Genomes analysis revealed that Fc gamma R-mediated phagocytosis and phagosome related pathways, which play a crucial role in efferocytosis, were significantly different between the 2 groups (Figure 2C). Consistently, in Gene Ontology analysis, genes related with actin cytoskeleton and actin filament markedly differed between the 2 groups (Figure 2D). During efferocytosis, macrophages dynamically transform their actin cytoskeleton to drive the engulfment of apoptotic cells and rely on actin filaments to form the filopodia.[25] The latter evidence prompted us to assess the role of ALDH2 in efferocytosis. To explore whether deletion of ALDH2 can affect efferocytosis by macrophages, we extracted primary peritoneal macrophages and BMDMs and co-cultured them with induced apoptotic VSMCs. Efferocytotic rate of ALDH2$^{-/-}$ primary peritoneal macrophages was lower than that of wild-type macrophages (34.0±1.1% versus 42.6±1.5%, *P*=0.0011; Figure 2E). Consistently, ALDH2$^{-/-}$ BMDMs showed lower efferocytotic activity compared with control group (26.4±1.5% versus 38.1±2.2%, *P*=0.0042; Figure 2F). Moreover, we used fluorescence microscopy to analyze efferocytosis and found that ALDH2$^{-/-}$ peritoneal macrophages showed decreased efferocytosis activity compared with ALDH2$^{+/+}$ macrophages (20.39±1.08% versus 36.41±3.27%, *P*=0.0006; Figure 2G). Next, using a living cell imaging system we observed that compared with ALDH2$^{-/-}$ macrophages, ALDH2 wild-type macrophages displayed greater phagocytotic activity (Videos S1 and S2). These data confirmed that bone marrow ALDH2 deletion dampened macrophage efferocytosis, which was primarily responsible for the accelerated progression of atherosclerosis in APOE$^{-/-}$ mice transplanted with APOE$^{-/-}$ALDH2$^{-/-}$ bone marrow.

ALDH2 Deletion in Macrophages Depresses Rac2 Expression and Activation During Efferocytosis Internalization

To explore the potential target proteins regulated by ALDH2 during efferocytosis, we stimulated primary peritoneal macrophages from ALDH2$^{-/-}$ or wild-type mice with induced apoptotic cells and performed mRNA sequencing.

Figure 2 Continued. B, Anti-monocyte+macrophage antibody (MOMA-2) and TUNEL staining of frozen sections of the tricuspid valve from APOE$^{-/-}$ mice transplanted with APOE$^{-/-}$ bone marrow and APOE$^{-/-}$ mice transplanted with APOE$^{-/-}$ALDH2$^{-/-}$ bone marrow which were fed with high-fat diet for 8 wk. Macrophage-associated apoptotic cells were TUNEL$^+$ debris (red) engulfed by MOMA-2$^+$ macrophages (green). Yellow * indicates macrophage-associated apoptotic cell and white * indicates free apoptotic cell (n=5). **C** and **D**, Primary ALDH2$^{+/+}$ and ALDH2$^{-/-}$ peritoneal macrophages were incubated with apoptotic cells and underwent mRNA-sequencing. Kyoto Encyclopedia of Genes and Genomes (KEGG) analysis and Gene Ontology (GO) analysis showed that efferocytosis-associated pathways and cellular components (red) were changed (n=3). **E** and **F**, Primary ALDH2$^{+/+}$ and ALDH2$^{-/-}$ peritoneal macrophages and bone-marrow derived macrophages (BMDMs) were incubated with apoptotic cells for 1.5 h and analyzed by flow cytometry (**E**, n=6; **F**, n=4). **G**, Primary peritoneal macrophages were incubated with stained apoptotic cells (red) for 1.5 h. After washing off free apoptotic cells, macrophages were stained with anti-F4/80 antibody (green) and observed using confocal microscopy (n=7). Data were shown as the mean±SE of mean and Student *t* test was used for statistical analysis, if not specifically indicated. As for TUNEL staining and efferocytosis in vivo, data were analyzed by Mann-Whitney test.

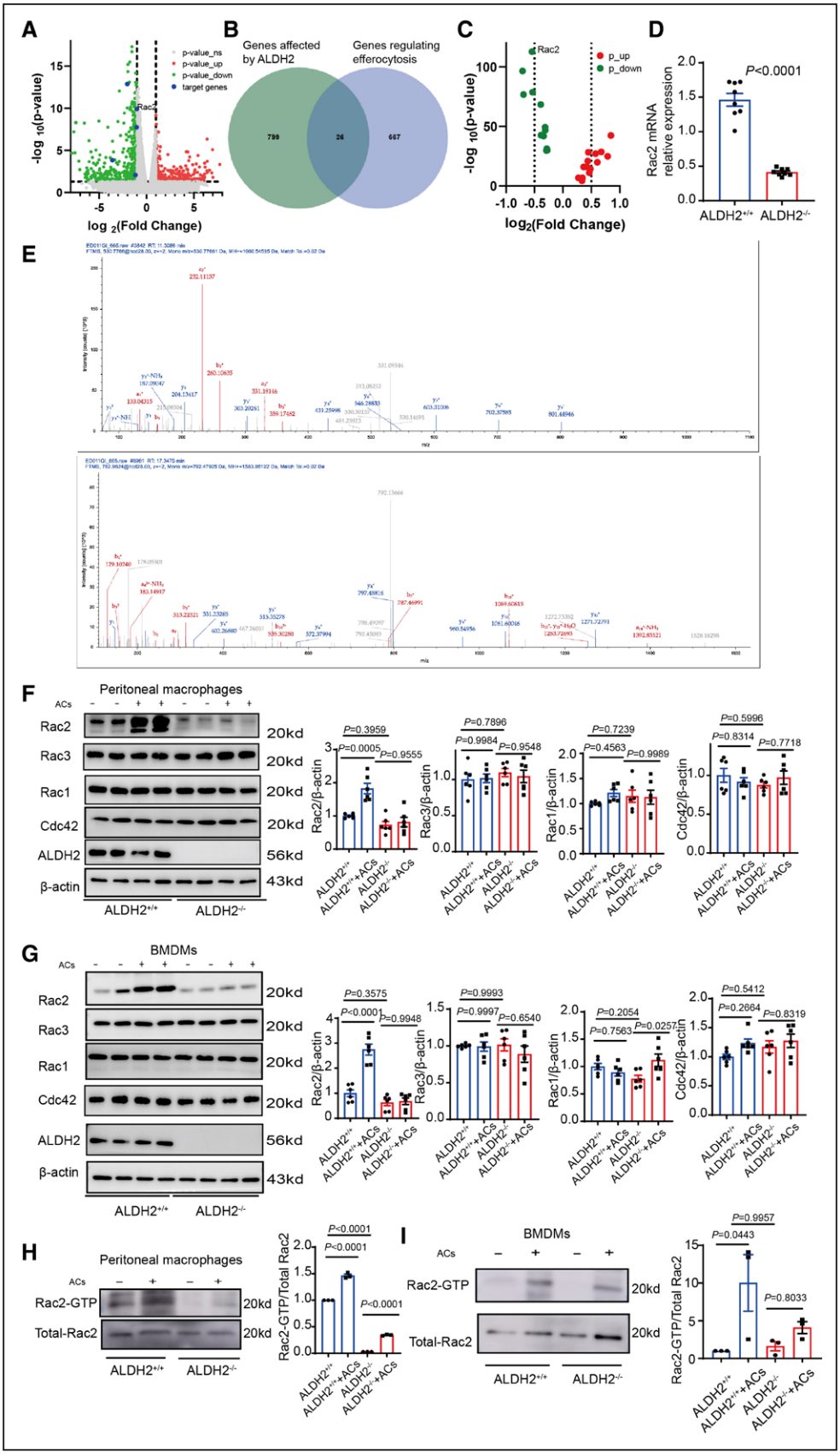

Figure 3. ALDH2 (aldehyde dehydrogenase 2) deletion in macrophages depresses Rac2 expression and activation during efferocytosis internalization. (*Continued*)

ALDH2 deficiency resulted in the downregulation of numerous efferocytosis-related genes, especially genes in Fc gamma R-mediated phagocytosis pathway (Figure 3A). Combining analysis of our results with the single-cell RNA sequencing results (GSE156234) in GEO database revealed that among the 26 efferocytosis-regulating genes altered by ALDH2 deletion, Rac2 showed the most statistically significant change (Figure 3B and 3C). Rac2 mRNA expression was downregulated in ALDH2$^{-/-}$ macrophages compared with wild-type macrophages when both were stimulated with apoptotic cells (Figure 3D). And subsequent proteomic analysis suggested that Rac2 interacted with ALDH2 (Figure 3E). Aforementioned results strongly suggested Rac2 was the downstream efferocytosis-regulating target affected by ALDH2 deficiency. Rac subfamily (Rac1, Rac2, Rac3) and Cdc42 are highly conserved small GTPases, which mediate actin dynamics in a parallel way. To verify whether Rac2 is the only Rac subfamily protein affected by ALDH2 deletion during efferocytosis, we investigated the aforementioned proteins by Western blotting. The expression of Rac2 was up-regulated in wild-type macrophages 30 minutes after apoptotic cells stimulation and maintained at a high level for 3 hours, while other Rac subfamily stayed relatively stable (Figure S1B). In the presence of ALDH2, Rac2 was up-regulated both in primary peritoneal macrophages and BMDMs during efferocytosis, and the upregulation of Rac2 vanished in the absence of ALDH2 (Figure 3F and 3G). The expression levels of other proteins remained unchanged (Figure 3F and 3G, Figure S1C and S1D). Consistently, Rac2 was activated to Rac2-GTP status during efferocytosis, and the activation of Rac2 was significantly impaired both in ALDH2$^{-/-}$ peritoneal macrophages and BMDMs compared with ALDH2$^{+/+}$ macrophages (Figure 3H and 3I). Therefore, our findings suggested that Rac2 was the downstream protein by which ALDH2 deletion or rs671 mutation affected efferocytosis.

Rac2 Plays a Crucial Role in Efferocytosis Internalization Stage and Overexpression of Rac2 in ALDH2$^{-/-}$ Macrophages Rescues Defected Efferocytosis

Considering that only Rac2 was up-regulated during efferocytosis internalization, we next explored whether Rac2 plays a more important role in efferocytosis in vivo and in vitro. To do so, we treated mice with dexamethasone to induce abundant thymocyte apoptosis, followed by apoptotic cell clearance by thymic macrophages. Dexamethasone-treated mice had increased Rac2 expression than those treated with PBS (Figure 4A), while ALDH2 did not alter between 2 groups (Figure S1E). Moreover, under laser scanning confocal microscopy, efferocytotic macrophages (macrophages which engulfed apoptotic cells) showed evidence of upregulation of Rac2 expression compared with nonefferocytotic macrophages (macrophages which did not engulf apoptotic cells), and in efferocytotic macrophages, Rac2 proteins clustered into dots (Figure 4B), suggesting that Rac2 played an important role during the process. To test whether Rac2 was essential for efferocytosis by macrophages, we transfected primary macrophages with siRNA-Rac2, that is, used siRNA to decrease Rac2 expression (Figure S1F through S1H), and then incubated them with induced apoptotic cells. In primary peritoneal macrophages, the efferocytotic rate of the siRNA-Rac2 group was lower than that of the siRNA-NC group (22.5±1.7% versus 31.2±2.3%, P=0.0357; Figure 4C). Similarly, in BMDMs, the efferocytotic activity of siRNA-Rac2 treated macrophages was markedly suppressed compared with siRNA-NC treated macrophages (27.7±0.8% versus 31.6±0.7%, P=0.0198; Figure 4D). To verify whether the decrease of efferocytotic activity of ALDH2 $^{-/-}$ macrophages is caused by downregulation of Rac2, we transfected BMDMs with Ad-Rac2 to overexpress Rac2 (Figure S1I). The efferocytotic rate of ALDH2$^{-/-}$ BMDMs transfected with Ad-Rac2 was markedly increased compared with that of ALDH2$^{-/-}$ BMDMs transfected with Ad-GFP (27.5±0.6% versus 19.4±0.9%, P=0.0002; Figure 4E), and nearly equal to that of ALDH2$^{+/+}$ BMDMs transfected with Ad-GFP (27.5±0.6% versus 24.3±0.8%, P=0.0640; Figure 4E). The efferocytotic rate of ALDH2$^{+/+}$ BMDMs transfected with Ad-Rac2 was similar to that of ALDH2$^{+/+}$ BMDMs transfected with Ad-GFP (26.7±0.7% versus 24.3±0.8%, P=0.1513; Figure 4E). Taken together, the observations revealed that Rac2 upregulation in macrophages is essential for sufficient efferocytosis internalization, and lack of Rac2 causes internalization dysfunction. ALDH2 deletion impaired macrophage efferocytosis via suppression of Rac2, while overexpression of Rac2 enhanced efferocytotic function of macrophages.

Figure 3 Continued. **A**–**C**, The Volcano plot and Venn diagram of mRNA sequencing and reanalysis of online data. Primary ALDH2$^{+/+}$ and ALDH2$^{-/-}$ peritoneal macrophages were incubated with apoptotic cells and underwent mRNA-sequencing (the same data set as in Figure 2E and 2F). We screened out efferocytosis-related genes affected by ALDH2 deletion, and extracted these gene-related data from the online data set. The online data set was analyzed by seruat package in R software. **D**, Relative mRNA expression of Rac2 in primary peritoneal macrophages stimulated with apoptotic cells (n=8). Data were from 3 or more independent experiments. **E**, Rac2 was identified in the protein mixture enriched by ALDH2 antibody. The upper graph represented peptide fragment CVVVGDGAVGK, and the lower graph represented peptide fragment KLAPITYPQGLALAK. The 2 fragments were specifically referred to Rac2 protein. **F** and **G**, Representative western blot images of target proteins (n=6), and Rac2 indicated total Rac2. Data were from 3 or more independent experiments. **H** and **I**, Representative Western blot images of Rac2-GTP and Rac2-total, standardized by Rac2-total (n=3). Data were from 3 or more independent experiments. Data were shown as the mean±SE of mean. Student *t* test was used for statistical analysis in Figure 3D, and one-way ANOVA was used in Figure 3F through 3I.

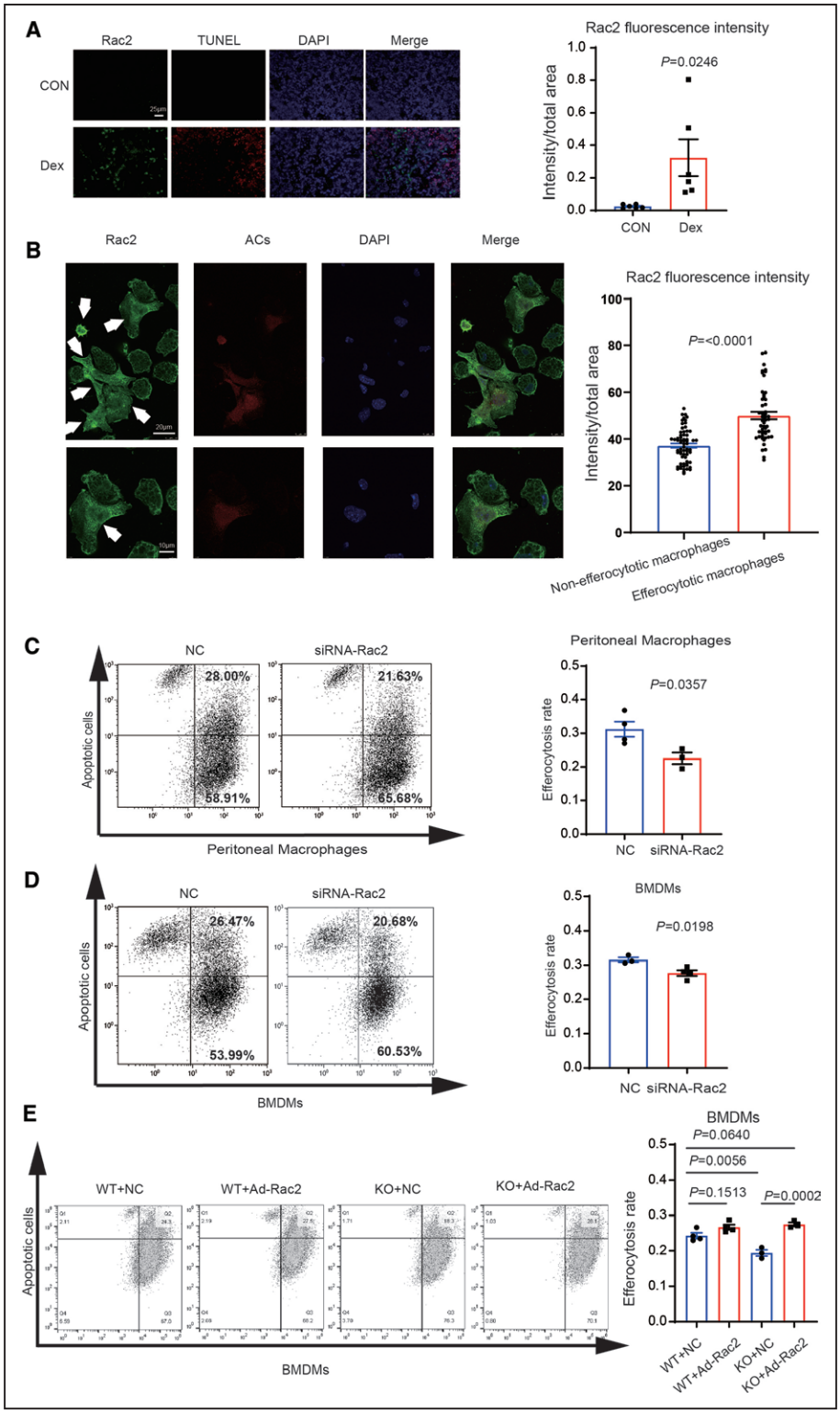

Figure 4. Rac2 plays a crucial role in efferocytosis internalization stage and overexpression of Rac2 in ALDH2$^{-/-}$ macrophages rescues defected efferocytosis.

A, Mice were injected intraperitoneally with PBS or 250 μg dexamethasone (Dex) for 18 h, and Rac2 immunostaining and TdT-mediated dUTP Nick-End Labeling (TUNEL) staining of thymic sections were performed. **B**, Confocal microscopy of macrophages treated with apoptotic cells (red) followed by labeling of Rac2 with Alexa-Fluor-488-conjugated secondary antibody (green). White arrows indicate efferocytotic macrophages. Data were from 3 or more independent experiments. **C** and **D**, Primary peritoneal ALDH2$^{+/+}$ macrophages and bone-marrow derived macrophages (BMDMs) were transfected with siRNA-Rac2 or NC (scrambled siRNA) and incubated with apoptotic cells for 1.5 h (n=3 or 4). Flow cytometry was used to analyze the efferocytotic rate. **E**, ALDH2$^{+/+}$ and ALDH2$^{-/-}$ BMDMs were transfected with NC (Ad-GFP) or Ad-Rac2 and incubated with apoptotic cells for 1.5 h. Flow cytometry was used to analyze the efferocytotic rate (n=3 or 4). Data were shown as the mean±SE of mean. Student *t* test was used for statistical analysis in Figure 4A through 4D, and 1-way ANOVA was used in Figure 4E and 4F.

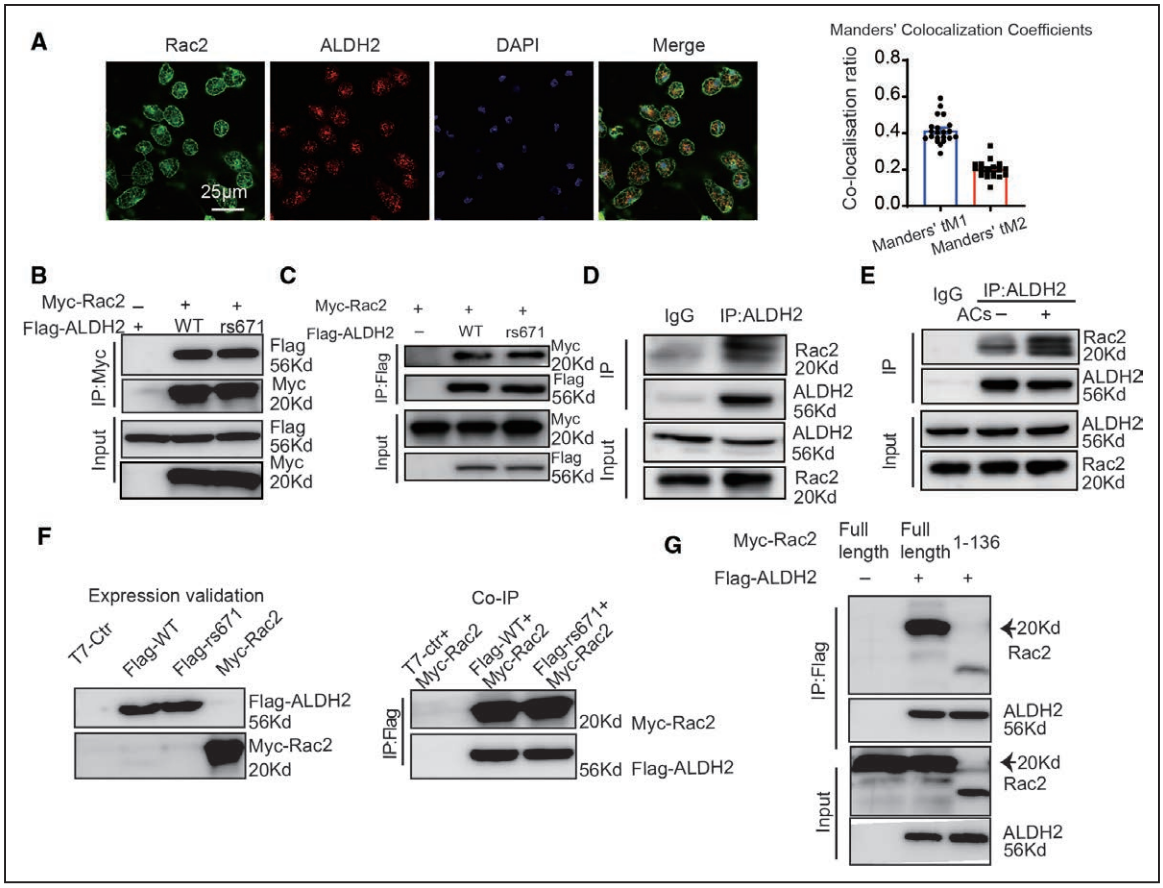

Figure 5. ALDH2 (aldehyde dehydrogenase 2) directly interacts with Rac2.
A, Colocalization of Rac2 (green) and ALDH2 (red) in primary peritoneal macrophages treated with apoptotic cells. Manders' tM1 represents the ratio of ALDH2 colocalized with Rac2 to total ALDH2, and Manders' tM2 represents the ratio of Rac2 colocalized with ALDH2 to total Rac2. **B** and **C**, Flag-ALDH2 or Flag-rs671 were co-transfected into HEK293T cells with Myc-Rac2. Cell lysates were subjected to co-immunoprecipitation (Co-IP) with anti-Flag or anti-Myc antibodies and followed by Western blotting. **D** and **E**, Co-IP was performed with lysates from RAW 264.7 macrophages (**D**) and primary peritoneal macrophages (**E**) treated with or without apoptotic cells. **F**, Myc-Rac2 and Flag-ALDH2 or Flag-rs671 were obtained by in vitro transcription and translation. The interaction between Rac2 and ALDH2 or rs671 mutant was assayed by Co-IP and Western blotting. **G**, Myc-Rac2 or its truncation mutants and Flag-ALDH2 were co-transfected into HEK293T cells. Cell lysates were subjected to Co-IP with anti-Flag antibodies and followed by Western blotting. Data were from 3 or more independent experiments.

ALDH2 Directly Interacts With Rac2

We performed high-resolution mass spectrometry-based proteomics to determine the mechanism of how ALDH2 influenced Rac2 expression. Rac2 was identified in the protein mixture enriched by ALDH2 antibody (Figure 3E), suggesting that these 2 proteins might interact with each other. Consistently, immunofluorescence and confocal microscopy analysis showed that a large portion of ALDH2 colocalized with Rac2 (Figure 5A). Then we transfected Flag-ALDH2 or Flag-rs671 with Myc-Rac2 into HEK293T cells, and in reciprocal coimmunoprecipitation assays observed that ALDH2 interacted with Rac2 (Figure 5B and 5C). Notably, rs671 mutant interacted with Rac2 in a fashion similar to that of wild-type ALDH2, which indicated that the enzyme activity of ALDH2 had limited role on the interaction with Rac2 (Figure 5B and 5C). Next, we found that endogenous ALDH2 and Rac2 interacted in RAW 264.7 macrophages and primary peritoneal macrophages (Figure 5D and 5E) and the level of interaction increased during efferocytosis (Figure 5E). Furthermore, we performed an in vitro binding assay with purified Flag-ALDH2 or Flag-rs671 and Myc-Rac2, and found that both ALDH2 and rs671 mutant interacted directly with Rac2 (Figure 5F). Domain mapping analysis revealed that ALDH2 interacted with Rac2 at the latter's region of amino acids 1 to 136 (Figure 5G). In summary, ALDH2 directly interacted with Rac2 during efferocytosis, independent of ALDH2 enzyme activity.

ALDH2 Stabilizes Rac2 by Attenuating Rac2 Ubiquitination

To explore the effect of ALDH2 or rs671 mutant on the stability of Rac2, we extracted primary peritoneal macrophages of APOE$^{-/-}$ and APOE$^{-/-}$ALDH2$^{-/-}$ mice and

 Arterioscler Thromb Vasc Biol. 2022;42:700–716. DOI: 10.1161/ATVBAHA.121.317204

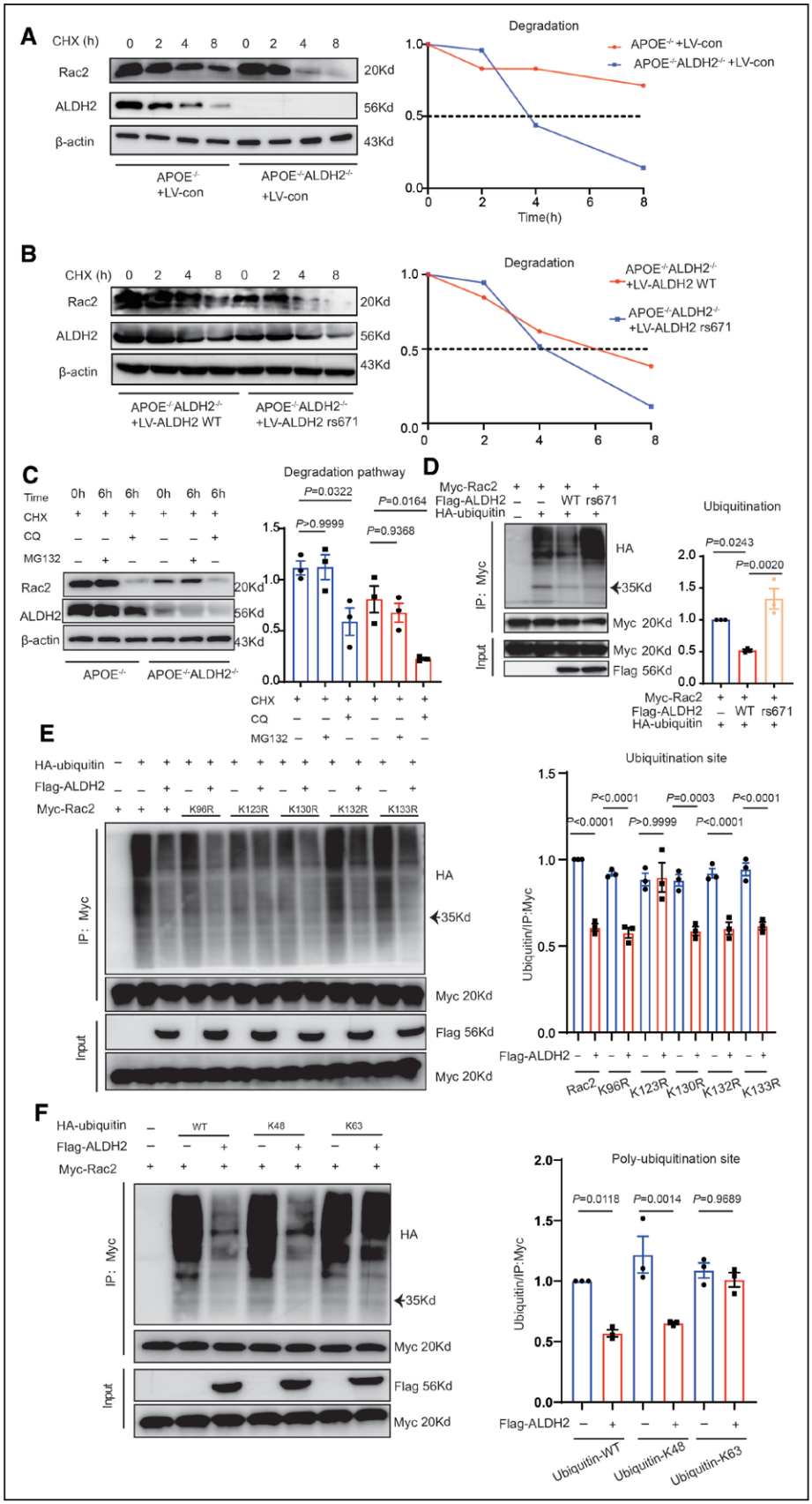

Figure 6. ALDH2 (aldehyde dehydrogenase 2) stabilizes Rac2 by attenuating Rac2 ubiquitination.
A and **B**, Primary peritoneal macrophages were transfected with LV-con or LV-ALDH2 or LV-rs671 and stimulated with apoptotic cells, subsequently followed by treatment of cycloheximide (CHX) for the indicated times. **C**, Primary peritoneal macrophages were (*Continued*)

infected macrophages with LV-ALDH2 or LV-rs671 or LV-con. We treated macrophages with the de novo protein synthesis inhibitor cycloheximide and measured the degradation of Rac2. The degradation of Rac2 was significantly increased in APOE$^{-/-}$ALDH2$^{-/-}$ macrophages compared with that in APOE$^{-/-}$ macrophages (Figure 6A). In ALDH2$^{-/-}$ macrophages, overexpression of ALDH2 WT rescued Rac2 degradation, but overexpression of ALDH2 rs671 mutant showed no benefits (Figure 6B). Next, we treated with primary macrophages with chloroquine or MG-132 to inhibit lysosomal or proteasome degradation pathway. Results showed that MG-132 treatment significantly reduced degradation of Rac2, while chloroquine treatment did not prevent its degradation, regardless of the presence of ALDH2. The results revealed that Rac2 mainly underwent proteasome degradation pathway (Figure 6C). To explore the reason ALDH2 and rs671 mutant play a different role in stabilization of Rac2, we co-transfected HEK293T cells with Myc-Rac2 and HA-ubiquitin with or without Flag-ALDH2 or Flag-rs671. We observed that ALDH2 WT led to a significant reduction in Rac2 ubiquitination, while rs671 mutant lost this function, compared with baseline (Figure 6D). To verify which ubiquitination site of Rac2 that ALDH2 modulated, we constructed K96R, K123R, K130R, K132R, and K133R of Rac2 and co-transfected with or without HA-ubiquitin and Flag-ALDH2. Results showed that K123R was resistant to ALDH2 modulating de-ubiquitination, which implied that ALDH2 mainly modulated the ubiquitination of Rac2 at lysine-123 (Figure 6E). To investigate the type of ALDH2-mediated polyubiquitination of Rac2, we used vectors expressing HA-tagged mutant ubiquitin (K48) and ubiquitin (K63), which contain substitution of arginine for all lysine residues except the lysine at position 48 or position 63, respectively. Results showed that ALDH2 significantly decreased K48-linked polyubiquitination rather than K63-linked polyubiquitination of Rac2. We confirmed that ALDH2 modulated K48-linked polyubiquitination of Rac2. Taken together, ALDH2 WT directly interacted with Rac2 and stabilized it by suppressing its K48-linked polyubiquitination at lysine-123 site.

ALDH2 rs671 Mutation in Human Macrophages Dampened the ACs-Induced Upregulation of Rac2 and Subsequent Efferocytosis

More importantly, to verify whether rs671 mutation in human decreases Rac2 expression during efferocytosis, we extracted PBMCs from healthy volunteers and stimulated them with apoptotic Jurkat cells. The characteristics of the volunteers are shown in Table S1. Results revealed that ALDH2 rs671 mutation did not alter the expression of Rac2 at baseline (Figure 7A). The expression of Rac2 in PBMCs from wild-type populations was up-regulated after being stimulated with apoptotic cells (Figure 7B). And during efferocytosis, PBMCs from ALDH2 rs671 mutation populations expressed less Rac2 protein, compared with those from ALDH2 wild-type populations (Figure 7C). More importantly, we co-cultured PBMCs with apoptotic Jurkat cells and found out that PBMCs from rs671 mutation displayed significantly lower efferocytotic ability compared with those from wild-type ones (8.6±1.3% versus 17.1±1.0%, $P<0.0001$; Figure 7D). To testify whether rescue of ALDH2-WT or ALDH2-rs671 expression in macrophages would restore efferocytotic ability, we transfected ALDH2$^{-/-}$ macrophages with LV-ALDH2-WT or LV-ALDH2-rs671 (Figure S1J). Results showed that supplement of ALDH2-WT rescued efferocytotic ability of ALDH2$^{-/-}$ macrophages to that of wild-type macrophages (31.0±1.2% versus 34.5±1.0%, $P=0.3307$; Figure 7E), but supplement of ALDH2-rs671 failed to make it (18.5±2.0% versus 34.5±1.0%, $P<0.0001$; Figure 7E).

DISCUSSION

The underlying mechanisms by which ALDH2 rs671 mutation causes elevated ACS incidence remain poorly defined. The present in vivo and in vitro study demonstrated that the ALDH2-Rac2-efferocytosis axis is critical for restraining formation of advanced plaques, thereby revealing a potential new therapeutic target. First, transplanting bone marrow from APOE$^{-/-}$ALDH2$^{-/-}$ to APOE$^{-/-}$ mice accelerated atherosclerosis and enlarged necrotic cores, accompanied by impaired macrophage efferocytotic activity both in vivo and in vitro. Second, ALDH2 deficiency and Rac2 deficiency caused the same defective macrophage efferocytosis. Supplement of wild-type ALDH2 or overexpression of Rac2 in ALDH2$^{-/-}$ macrophages rescued the dampened efferocytosis. Finally, using RNA-seq and proteomics, and subsequent co-immunoprecipitation assay, we showed that ALDH2 directly interacted with Rac2 in the 1-136 region of the latter, and regulated the K48-linked polyubiquitination at lysine 123 site (Figure 8, Graphic Abstract).

Figure 6 Continued. treated with CHX, and stimulated with MG-132 or chloroquine (CQ) for the indicated time. **D**, HEK293T cells were transfected with Myc-Rac2 and HA-Ub, with or without Flag-ALDH2 or Flag-rs671. Cell lysates were collected, and Co-IP assays were performed. **E**, HEK293T cells were transfected with HA-Ub and Myc-Rac2 or its single site mutation, with or without Flag-ALDH2. Cell lysates were collected, and Co-IP assays were performed. The red bars referred to groups transfected with Flag-ALDH2 plasmid and blue bars referred to groups transfected without Flag-ALDH2 plasmids. **F**, HEK293T cells were transfected with Myc-Rac2 and HA-Ub or K48 or K63, with or without Flag-ALDH2. Cell lysates were collected, and Co-IP assays were performed. The red bars referred to groups transfected with Flag-ALDH2 plasmid and blue bars referred to groups transfected without Flag-ALDH2 plasmids. Data were shown as the mean±SE of mean. One-way ANOVA was used for statistical analysis in Figure 6C through 6F. Data were from 3 or more independent experiments.

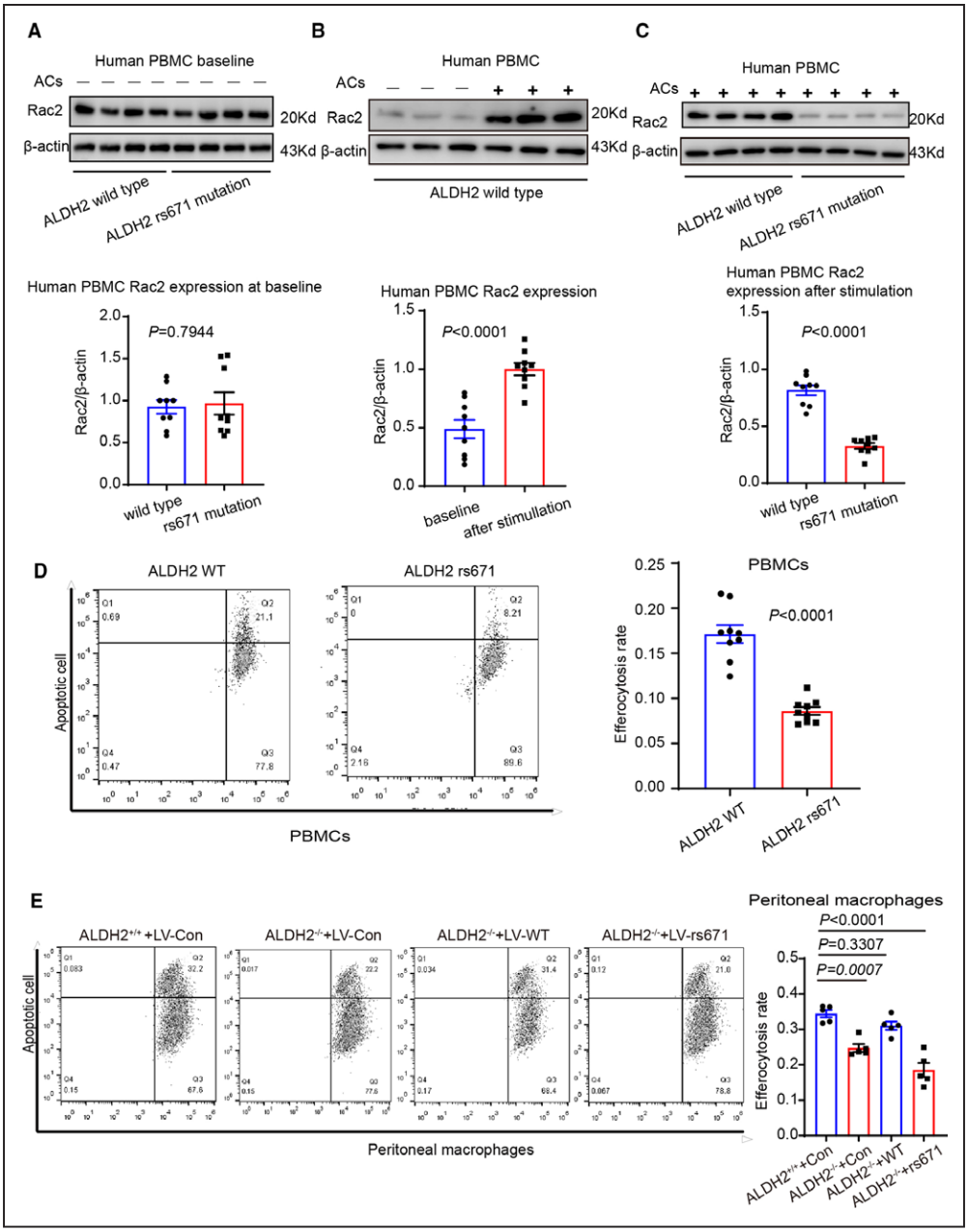

Figure 7. ALDH2 (aldehyde dehydrogenase 2) rs671 mutation in human macrophages dampened the apoptotic cells (ACs)-induced upregulation of Rac2 and subsequent efferocytosis.
A–**C**, Human peripheral blood mononuclear cells (PBMCs) from healthy volunteers were stimulated with apoptotic Jurkat cells and underwent Western blotting. **D**, Human PBMCs were incubated with apoptotic Jurkat cells and underwent flow cytometry. **E**, Primary peritoneal macrophages from ALDH2$^{-/-}$ mice were transfected with LV-con, LV-WT or LV-rs671, and incubated with apoptotic vascular smooth muscle cells (VSMCs) and underwent flow cytometry. Data were shown as the mean±SE of mean. Student *t* test was used for statistical analysis in Figure 7A through 7D, and 1-way ANOVA was used for statistical analysis in Figure 7E.

Because therapeutic strategies based on the finding and binding stages of efferocytosis are limited by side effects, interest has shifted to targeting the internalization and degradation stage. Collectively, data from our current study showed a beneficial role of ALDH2 in macrophages in terms of cardiovascular artery disease. Interestingly, ALDH2 deficiency showed exactly the opposite role in a different kind of cardiovascular disease, with evidence from both basic science experiments and clinical trials. On the one hand, ALDH2 deficiency has been demonstrated to increase mitochondrial injury, reactive aldehyde production, and the accumulation of reactive oxygen species, leading to susceptibility to myocardial infarction and coronary artery disease.[12,13,26–28] On the other hand, ALDH2 deficiency suppresses VSMC phenotypic switch and ultimately prevents the incidence of abdominal aortic dissection, showing a protective role of ALDH2 deficiency.[8] Therefore, targeting ALDH2 in a tissue specific

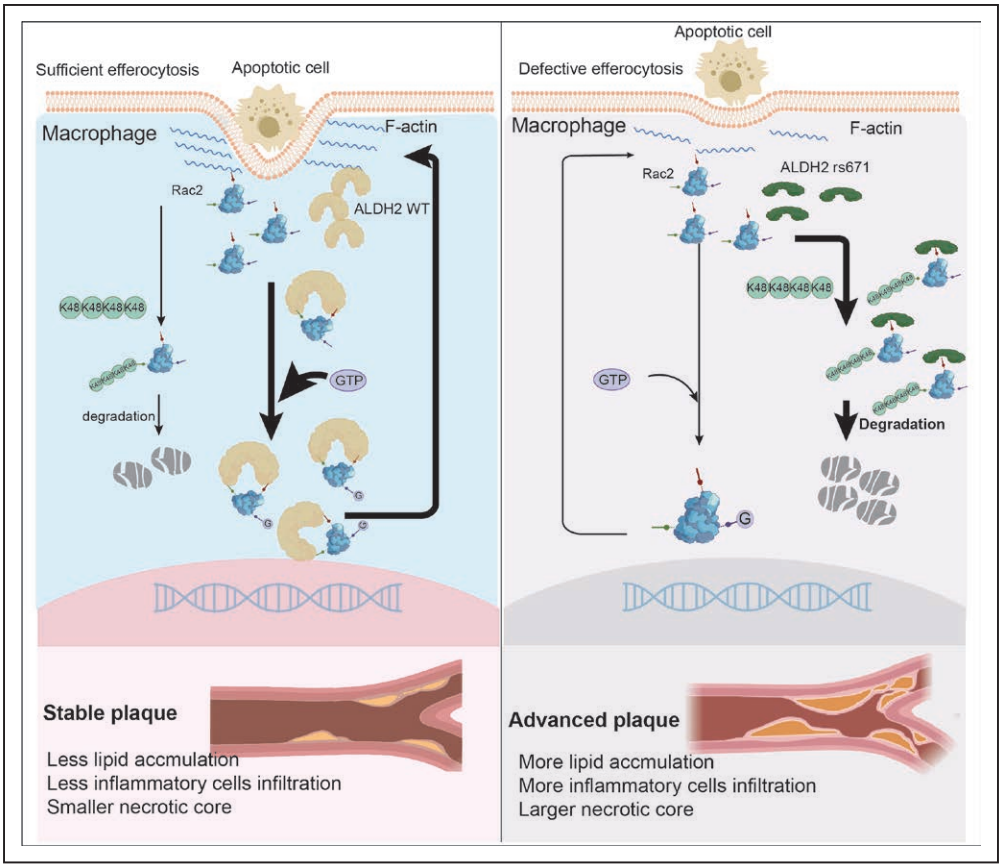

Figure 8. ALDH2 (aldehyde dehydrogenase 2) enhances macrophage efferocytosis by attenuating Rac2 ubiquitination. Wild-type ALDH2 directly interacted with Rac2 and regulated K48-linked polyubiquitination of the latter at K123, and prevented Rac2 from degradation. Subsequently, wild-type ALDH2 enhanced efferocytotic ability by availing phagocytotic cup formation.

manner or targeting the key downstream proteins may be potential approaches to balance the double-edged sword role of ALDH2 deficiency. As for atherosclerosis prevention targeting macrophages, inhibiting foam cell formation to lower lipids accumulation and enhancing efferocytosis to clear necrotic debris in lesion area are 2 major approaches. A previous study showed that AMPK-phosphorylated ALDH2 translocated to the nucleus and repressed the expression of ATP6V0E2 in absence of LDLR (low-density lipoprotein receptor), and subsequently inhibited macrophage lysosomal function, endocytosis and autophagy. Results from the current study clearly showed that ALDH2 directly interacted with and stabilized Rac2 from degradation and subsequently enhanced efferocytosis, rendering rescue of Rac2 expression in the rs671 mutant populations potentially beneficial. Taken together, we believe that rescuing autophagy and efferocytosis targeting macrophage ATP6V0E2 and Rac2 are both promising for atherosclerosis prevention, especially for rs671 mutation populations.

The small GTPase Rac family members are essential for efferocytosis, which regulates the rearrangements of actin and membrane.[29] However, previous studies mostly focused on Rac1, and only 2 studies mentioned the role of Rac2 in efferocytosis.[30–34] During efferocytosis, the expression of Rac1 remains unchanged, only its activity is elevated.[30–32] Although Rac1 and Rac2 share 92% sequence identity, they differ in many aspects.[35] Rac1 is ubiquitously expressed throughout the body, while Rac2 is a hematopoietic-specific protein.[35] Emerging evidence shows that Rac2 displays a specific, nonredundant role in hematopoietic cells and discriminates itself from the ubiquitous Rac1.[35–37] The previous study involving Rac2 during efferocytosis showed an increase of total Rac protein expression level, but they did not verify which member it was.[33] Our results revealed that only the expression of Rac2 was elevated during efferocytosis, while that of Rac1, Rac3, and Cdc42 remained unchanged. More importantly, efferocytotic macrophages displayed a significantly higher expression of Rac2 compared with nonefferocytotic macrophages. The results underscored that Rac2 plays a more significant role in efferocytosis. The ensuing inhibition and rescue experiments showed that without interfering with others, solely controlling the expression of Rac2 significantly regulated macrophage efferocytosis. These results cast new light on the mechanisms regulating efferocytosis and provide a novel research direction for small GTPase Rac family proteins.

Engulfment of apoptotic cells and debris by efferocytosis depends on the ability of macrophages to generate

phagocytosis cups, which are the rings or ruffles of actin-driven protrusion encircling nonprotrusive domains. To effectively capture and internalize the apoptotic cells and debris, macrophages rely on the presence and activity of multiple small GTPases, such as the Rac family proteins, to polymerize actin to form the phagocytosis cup.[36–38] Rac1 is the shining star among small GTPases, and it is valid that the switch between Rac1-GDP and Rac1-GTP status regulates dynamics of actin, which contributes to efferocytosis.[31,32,39] Rac3 may play a role in macrophage phagocytosis of microbes[40,41] but few studies focus on its functions on efferocytosis. As for Cdc42, studies showed that it was not involved in apoptotic cell internalization, but it assisted RvD1-mediated efferocytosis.[42]

Previous studies showed that Hector 1 and other E3 ligases regulated Rac2 ubiquitination and thus affected its function.[43] However, deubiquitination of Rac2 was rarely reported. Our study innovatively found that ALDH2 can significantly reduce K48-linked polyubiquitination at K123 site of Rac2, leading to enhanced protein stability. We posited that ALDH2 may influence the binding of other E3 ligases or deubiquitinating enzymes to Rac2 by directly interacting with it, or changing the conformation of Rac2, thereby affecting its ubiquitination level. Furthermore, our results also addressed the confusion on why ALDH2 knockout in mice and rs671 mutation in humans resulted in the same outcome in the setting of atherosclerosis. Together, these findings explained the results of our clinical studies, in which we determined that the ALDH2 mutation was a genetic risk factor for ACS and predicted a worse prognosis of those patients. Moreover, our results underscored the critical role of ALDH2 and Rac2 in macrophage activity to clear apoptotic cells and debris and provided potential targets to enhance macrophage efferocytosis for regressing atherosclerosis and stabilizing plaque, especially in rs671 mutation carriers.

In conclusion, our study uncovered a new pathway about ALDH2 reduced atherosclerosis formation and protected humans from ACS incidence. ALDH2 directly interacted with and stabilized Rac2, subsequently inhibiting the K48-linked polyubiquitination at the K123 site of the latter. ALDH2 rs671 mutation lost the protective function and increased the degradation of Rac2, suppressing macrophage efferocytosis and aggravating atherosclerosis. Our finding provided potential therapeutic targets for atherosclerosis prevention, especially for rs671 mutation populations.

ARTICLE INFORMATION

Received November 10, 2021; accepted March 16, 2022.

Affiliations

Department of Emergency Medicine (J.Z., X.Z., Y.G., S.W., Q.Y., W.S., S.C., T.X., K.Y., J.G., C.P., J.W., J.P., T.H., Y.C., F.X.), Chest Pain Center (J.Z., X.Z., Y.G., S.W., Q.Y., W.S., S.C., T.X., K.Y., J.G., C.P., J.W., J.P., T.H., Y.C., F.X.), Shandong Provincial Clinical Research Center for Emergency and Critical Care Medicine, Institute of Emergency and Critical Care Medicine of Shandong University (J.Z., X.Z., Y.G., S.W., Q.Y., W.S., S.C., T.X., K.Y., J.G., C.P., J.W., J.P., T.H., Y.C., F.X.), Key Laboratory of Emergency and Critical Care Medicine of Shandong Province, Key Laboratory of Cardiopulmonary-Cerebral Resuscitation Research of Shandong Province, Shandong Provincial Engineering Laboratory for Emergency and Critical Care Medicine (J.Z., X.Z., Y.G., S.W., Q.Y., W.S., S.C., T.X., K.Y., J.G., C.P., J.W., J.P., T.H., Y.C., F.X.), and The Key Laboratory of Cardiovascular Remodeling and Function Research, Chinese Ministry of Education, Chinese Ministry of Health and Chinese Academy of Medical Sciences; The State and Shandong Province Joint Key Laboratory of Translational Cardiovascular Medicine (J.Z., X.Z., Y.G., S.W., Q.Y., W.S., S.C., T.X., K.Y., J.G., C.P., J.W., J.P., T.H., Y.C., F.X.), Qilu Hospital, Shandong University, Jinan, China. Center of Intelligent Medical Engineering, School of Control Science and Engineering, Shandong University, Jinan, China (Z.L., H.S.).

Acknowledgments

We would like to acknowledge the help from Huan Tao at Vanderbilt University School of Medicine, Nashville, for valuable suggestions about the experiment. All animal procedures were in accordance with the National Institutes of Health Guidelines for the care and use of laboratory animals and were approved by the Animal Use and Care Committee of Shandong University. All human samples were collected by Qilu Hospital, and human experiments were approved by Institutional Medical Ethics Committees of Qilu Hospital. Informed consent was obtained from all participants.

Sources of Funding

This work was supported by the National Natural Science Foundation of China [82072144, 81873950, 81772036, 81873953], the State Key Program of the National Natural Science Foundation of China [82030059], Taishan Young Scholar Program of Shandong Province [tsqn20161065, tsqn201812129], Taishan Pandeng Scholar Program of Shandong Province [tspd20181220], National S&T Fundamental Resources Investigation Project [2018FY100600, 2018FY100602], National Key R&D Program of China [2020YFC1512700, 2020YFC1512705, 2020YFC1512703], the Interdisciplinary Young Researcher Groups Program of Shandong University [2020QNQT004], Clinical Research Center of Shandong University [2020SDUCRCB003].

Disclosures

None.

Supplemental Material

Table S1
Figure S1
Major Resources Table
Movie S1 and S2

REFERENCES

1. Libby P, Bornfeldt KE, Tall AR. Atherosclerosis: successes, surprises, and future challenges. *Circ Res*. 2016;118:531–534. doi: 10.1161/CIRCRESAHA.116.308334
2. Seneviratne AN, Edsfeldt A, Cole JE, Kassiteridi C, Swart M, Park I, Green P, Khoyratty T, Saliba D, Goddard ME, et al. Interferon regulatory factor 5 controls necrotic core formation in atherosclerotic lesions by impairing efferocytosis. *Circulation*. 2017;136:1140–1154. doi: 10.1161/CIRCULATIONAHA.117.027844
3. Barrett TJ. Macrophages in atherosclerosis regression. *Arterioscler Thromb Vasc Biol*. 2020;40:20–33. doi: 10.1161/ATVBAHA.119.312802
4. Doran AC, Yurdagul A Jr, Tabas I. Efferocytosis in health and disease. *Nat Rev Immunol*. 2020;20:254–267. doi: 10.1038/s41577-019-0240-6
5. Koelwyn GJ, Corr EM, Erbay E, Moore KJ. Regulation of macrophage immunometabolism in atherosclerosis. *Nat Immunol*. 2018;19:526–537. doi: 10.1038/s41590-018-0113-3
6. Kojima Y, Volkmer JP, McKenna K, Civelek M, Lusis AJ, Miller CL, Direnzo D, Nanda V, Ye J, Connolly AJ, et al. CD47-blocking antibodies restore phagocytosis and prevent atherosclerosis. *Nature*. 2016;536:86–90. doi: 10.1038/nature18935
7. Kato N, Takeuchi F, Tabara Y, Kelly TN, Go MJ, Sim X, Tay WT, Chen CH, Zhang Y, Yamamoto K, et al. Meta-analysis of genome-wide association studies identifies common variants associated with blood pressure variation in east Asians. *Nat Genet*. 2011;43:531–538. doi: 10.1038/ng.834
8. Yang K, Ren J, Li X, Wang Z, Xue L, Cui S, Sang W, Xu T, Zhang J, Yu J, et al. Prevention of aortic dissection and aneurysm via an ALDH2-mediated switch

in vascular smooth muscle cell phenotype. *Eur Heart J.* 2020;41:2442–2453. doi: 10.1093/eurheartj/ehaa352
9. Bartoli-Leonard F, Saddic L, Aikawa E. Double-edged sword of ALDH2 mutations: one polymorphism can both benefit and harm the cardiovascular system. *Eur Heart J.* 2020;41:2453–2455. doi: 10.1093/eurheartj/ehaa444
10. Millwood IY, Walters RG, Mei XW, Guo Y, Yang L, Bian Z, Bennett DA, Chen Y, Dong C, Hu R, et al; China Kadoorie Biobank Collaborative Group. Conventional and genetic evidence on alcohol and vascular disease aetiology: a prospective study of 500 000 men and women in China. *Lancet.* 2019;393:1831–1842. doi: 10.1016/S0140-6736(18)31772-0
11. Chen CH, Ferreira JC, Gross ER, Mochly-Rosen D. Targeting aldehyde dehydrogenase 2: new therapeutic opportunities. *Physiol Rev.* 2014;94:1–34. doi: 10.1152/physrev.00017.2013
12. Pan C, Zhao Y, Bian Y, Shang R, Wang JL, Xue L, Wei SJ, Zhang H, Chen YG, Xu F. Aldehyde dehydrogenase 2 Glu504Lys variant predicts a worse prognosis of acute coronary syndrome patients. *J Cell Mol Med.* 2018;22:2518–2522. doi: 10.1111/jcmm.13536
13. Xu F, Chen YG, Xue L, Li RJ, Zhang H, Bian Y, Zhang C, Lv RJ, Feng JB, Zhang Y. Role of aldehyde dehydrogenase 2 Glu504lys polymorphism in acute coronary syndrome. *J Cell Mol Med.* 2011;15:1955–1962. doi: 10.1111/j.1582-4934.2010.01181.x
14. Zhang G, Li C, Zhu N, Chen Y, Yu Q, Liu E, Wang R. Sex differences in the formation of atherosclerosis lesion in apoE-/-mice and the effect of 17β-estrodiol on protein S-nitrosylation. *Biomed Pharmacother.* 2018;99:1014–1021. doi: 10.1016/j.biopha.2018.01.145
15. Daugherty A, Tall AR, Daemen MJAP, Falk E, Fisher EA, García-Cardeña G, Lusis AJ, Owens AP 3rd, Rosenfeld ME, Virmani R; American Heart Association Council on Arteriosclerosis, Thrombosis and Vascular Biology; and Council on Basic Cardiovascular Sciences. Recommendation on design, execution, and reporting of animal atherosclerosis studies: a scientific statement from the american heart association. *Arterioscler Thromb Vasc Biol.* 2017;37:e131–e157. doi: 10.1161/ATV.0000000000000062
16. Robinet P, Milewicz DM, Cassis LA, Leeper NJ, Lu HS, Smith JD. Consideration of sex differences in design and reporting of experimental arterial pathology studies-statement from ATVB council. *Arterioscler Thromb Vasc Biol.* 2018;38:292–303. doi: 10.1161/ATVBAHA.117.309524
17. Edgar L, Akbar N, Braithwaite AT, Krausgruber T, Gallart-Ayala H, Bailey J, Corbin AL, Khoyratty TE, Chai JT, Alkhalil M, et al. Hyperglycemia induces trained immunity in macrophages and their precursors and promotes atherosclerosis. *Circulation.* 2021;144:961–982. doi: 10.1161/CIRCULATIONAHA.120.046464
18. Que X, Hung MY, Yeang C, Gonen A, Prohaska TA, Sun X, Diehl C, Määttä A, Gaddis DE, Bowden K, et al. Oxidized phospholipids are proinflammatory and proatherogenic in hypercholesterolaemic mice. *Nature.* 2018;558:301–306. doi: 10.1038/s41586-018-0198-8
19. Anandan V, Thulaseedharan T, Suresh Kumar A, Chandran Latha K, Revikumar A, Mullasari A, Kartha CC, Jaleel A, Ramachandran S. Cyclophilin a impairs efferocytosis and accelerates atherosclerosis by overexpressing CD 47 and down-regulating calreticulin. *Cells.* 2021;10:3598. doi: 10.3390/cells10123598
20. Kojima Y, Downing K, Kundu R, Miller C, Dewey F, Lancero H, Raaz U, Perisic L, Hedin U, Schadt E, et al. Cyclin-dependent kinase inhibitor 2B regulates efferocytosis and atherosclerosis. *J Clin Invest.* 2019;129:2164. doi: 10.1172/JCI129277
21. Le TS, Takahashi M, Isozumi N, Miyazato A, Hiratsuka Y, Matsumura K, Taguchi T, Maenosono S. Quick and mild isolation of intact lysosomes using magnetic-plasmonic hybrid nanoparticles. *ACS Nano.* 2022;16:885–896. doi: 10.1021/acsnano.1c08474
22. Manders EMM, Verbeek FJ, Aten JA. Measurement of co-localization of objects in dual-colour confocal images. *J Microsc.* 1993;169:375–382. doi: 10.1111/j.1365-2818.1993.tb03313.x
23. Lantz C, Radmanesh B, Liu E, Thorp EB, Lin J. Single-cell RNA sequencing uncovers heterogenous transcriptional signatures in macrophages during efferocytosis. *Sci Rep.* 2020;10:14333. doi: 10.1038/s41598-020-70353-y
24. Satija R, Farrell JA, Gennert D, Schier AF, Regev A. Spatial reconstruction of single-cell gene expression data. *Nat Biotechnol.* 2015;33:495–502. doi: 10.1038/nbt.3192
25. Davidson AJ, Wood W. Macrophages use distinct actin regulators to switch engulfment strategies and ensure phagocytic plasticity in vivo. *Cell Rep.* 2020;31:107692. doi: 10.1016/j.celrep.2020.107692
26. Pan C, Xing JH, Zhang C, Zhang YM, Zhang LT, Wei SJ, Zhang MX, Wang XP, Yuan QH, Xue L, et al. Aldehyde dehydrogenase 2 inhibits inflammatory response and regulates atherosclerotic plaque. *Oncotarget.* 2016;7:35562–35576. doi: 10.18632/oncotarget.9384
27. Zhong S, Li L, Zhang YL, Zhang L, Lu J, Guo S, Liang N, Ge J, Zhu M, Tao Y, et al. Acetaldehyde dehydrogenase 2 interactions with LDLR and AMPK regulate foam cell formation. *J Clin Invest.* 2019;129:252–267. doi: 10.1172/JCI122064
28. Takagi S, Iwai N, Yamauchi R, Kojima S, Yasuno S, Baba T, Terashima M, Tsutsumi Y, Suzuki S, Morii I, et al. Aldehyde dehydrogenase 2 gene is a risk factor for myocardial infarction in Japanese men. *Hypertens Res.* 2002;25:677–681. doi: 10.1291/hypres.25.677
29. Diring J, Mouilleron S, McDonald NQ, Treisman R. RPEL-family rhoGAPs link Rac/Cdc42 GTP loading to G-actin availability. *Nat Cell Biol.* 2019;21:845–855. doi: 10.1038/s41556-019-0337-y
30. Tao H, Yancey PG, Babaev VR, Blakemore JL, Zhang Y, Ding L, Fazio S, Linton MF. Macrophage SR-BI mediates efferocytosis via Src/PI3K/Rac1 signaling and reduces atherosclerotic lesion necrosis. *J Lipid Res.* 2015;56:1449–1460. doi: 10.1194/jlr.M056689
31. Yurdagul A Jr, Subramanian M, Wang X, Crown SB, Ilkayeva OR, Darville L, Kolluru GK, Rymond CC, Gerlach BD, Zheng Z, et al. Macrophage metabolism of apoptotic cell-derived arginine promotes continual efferocytosis and resolution of injury. *Cell Metab.* 2020;31:518–533.e10. doi: 10.1016/j.cmet.2020.01.001
32. Proto JD, Doran AC, Gusarova G, Yurdagul A, Jr., Sozen E, Subramanian M, Islam MN, Rymond CC, Du J, Hook J, et al. Regulatory T cells promote macrophage efferocytosis during inflammation resolution. *Immunity.* 2018;49:666–677 e666. doi: 10.1016/j.immuni.2018.07.015
33. Xiao H, Wang H, Silva EA, Thompson J, Guillou A, Yates JR Jr, Buchon N, Franc NC. The Pallbearer E3 ligase promotes actin remodeling via RAC in efferocytosis by degrading the ribosomal protein S6. *Dev Cell.* 2015;32:19–30. doi: 10.1016/j.devcel.2014.11.015
34. Cuttell L, Vaughan A, Silva E, Escaron CJ, Lavine M, Van Goethem E, Eid JP, Quirin M, Franc NC. Undertaker, a Drosophila Junctophilin, links Draper-mediated phagocytosis and calcium homeostasis. *Cell.* 2008;135:524–534. doi: 10.1016/j.cell.2008.08.033
35. Baier A, Ndoh VN, Lacy P, Eitzen G. Rac1 and Rac2 control distinct events during antigen-stimulated mast cell exocytosis. *J Leukoc Biol.* 2014;95:763–774. doi: 10.1189/jlb.0513281
36. Hoppe AD, Swanson JA. Cdc42, Rac1, and Rac2 display distinct patterns of activation during phagocytosis. *Mol Biol Cell.* 2004;15:3509–3519. doi: 10.1091/mbc.e03-11-0847
37. Hsu AP, Donkó A, Arrington ME, Swamydas M, Fink D, Das A, Escobedo O, Bonagura V, Szabolcs P, Steinberg HN, et al. Dominant activating RAC2 mutation with lymphopenia, immunodeficiency, and cytoskeletal defects. *Blood.* 2019;133:1977–1988. doi: 10.1182/blood-2018-11-886028
38. Buckley CM, Pots H, Gueho A, Vines JH, Munn CJ, Phillips BA, Gilsbach B, Traynor D, Nikolaev A, Soldati T, et al. Coordinated Ras and Rac activity shapes macropinocytic cups and enables phagocytosis of geometrically diverse bacteria. *Curr Biol.* 2020;30:2912–2926 e2915. doi: 10.1016/j.cub.2020.05.049
39. Viaud M, Ivanov S, Vujic N, Duta-Mare M, Aira LE, Barouillet T, Garcia E, Orange F, Dugail I, Hainault I, et al. Lysosomal cholesterol hydrolysis couples efferocytosis to anti-inflammatory oxysterol production. *Circ Res.* 2018;122:1369–1384. doi: 10.1161/CIRCRESAHA.117.312333
40. Ueyama T, Eto M, Kami K, Tatsuno T, Kobayashi T, Shirai Y, Lennartz MR, Takeya R, Sumimoto H, Saito N. Isoform-specific membrane targeting mechanism of Rac during Fc gamma R-mediated phagocytosis: positive charge-dependent and independent targeting mechanism of Rac to the phagosome. *J Immunol.* 2005;175:2381–2390. doi: 10.4049/jimmunol.175.4.2381
41. Miyano K, Sumimoto H. Assessment of the role for Rho family GTPases in NADPH oxidase activation. *Methods Mol Biol.* 2012;827:195–212. doi: 10.1007/978-1-61779-442-1_14
42. Gerlach BD, Marinello M, Heinz J, Rymut N, Sansbury BE, Riley CO, Sadhu S, Hosseini Z, Kojima Y, Tang DD, et al. Resolvin D1 promotes the targeting and clearance of necroptotic cells. *Cell Death Differ.* 2020;27:525–539. doi: 10.1038/s41418-019-0370-1
43. Kogler M, Tortola L, Negri GL, Leopoldi A, El-Naggar AM, Mereiter S, Gomez-Diaz C, Nitsch R, Tortora D, Kavirayani AM, et al. HACE1 prevents lung carcinogenesis via inhibition of Rac-family GTPases. *Cancer Res.* 2020;80:3009–3022. doi: 10.1158/0008-5472.CAN-19-2270